Biochimica et Biophysica Acta 1832 (2013) 1697–1707

Contents lists available at SciVerse ScienceDirect

Biochimica et Biophysica Acta

journal homepage: www.elsevier.com/locate/bbadis

# Suppression of tumorigenicity by MicroRNA-138 through inhibition of EZH2-CDK4/6-pRb-E2F1 signal loop in glioblastoma multiforme

Shuwei Qiu [a,1], Daquan Huang [a,1], Deling Yin [b], Fangcheng Li [c], Xiangping Li [d], Hsiang-fu Kung [e], Ying Peng [a,*]

[a] Department of Neurology, The Sun Yat-sen Memorial Hospital, Sun Yat-sen University, Guangzhou, China
[b] Department of Internal Medicine, College of Medicine, East Tennessee State University, Johnson City, Tennessee, USA
[c] Department of Neurosurgery, The Sun Yat-sen Memorial Hospital, Sun Yat-sen University, Guangzhou, China
[d] Department of Otolaryngology-Head and Neck Surgery, Nanfang Hospital, Southern Medical University, Guangzhou, China
[e] Laboratory of Integrated Biosciences, School of Life Sciences, Sun Yat-sen University, Guangzhou, China

ARTICLE INFO

*Article history:*
Received 31 December 2012
Received in revised form 5 May 2013
Accepted 13 May 2013
Available online 22 May 2013

*Keywords:*
Glioblastoma multiforme/microRNA-138/EZH2/CDK6/tumorigenicity/TCGA

ABSTRACT

Deregulation of microRNAs (miRNAs) is implicated in tumor progression. We attempt to indentify the tumor suppressive miRNA not only down-regulated in glioblastoma multiforme (GBM) but also potent to inhibit the oncogene EZH2, and then investigate the biological function and pathophysiologic role of the candidate miRNA in GBM. In this study, we show that miRNA-138 is reduced in both GBM clinical specimens and cell lines, and is effective to inhibit EZH2 expression. Moreover, high levels of miR-138 are associated with long overall and progression-free survival of GBM patients from The Cancer Genome Atlas dataset (TCGA) data portal. Ectopic expression of miRNA-138 effectively inhibits GBM cell proliferation *in vitro* and tumorigenicity *in vivo* through inducing cell cycles G1/S arrest. Mechanism investigation reveals that miRNA-138 acquires tumor inhibition through directly targeting EZH2, CDK6, E2F2 and E2F3. Moreover, an EZH2-mediated signal loop, EZH2-CDK4/6-pRb-E2F1, is probably involved in GBM tumorigenicity, and this loop can be blocked by miRNA-138. Additionally, miRNA-138 negatively correlates to mRNA levels of EZH2 and CDK6 among GBM clinical samples from both TCGA and our small amount datasets. In conclusion, our data demonstrate a tumor suppressive role of miRNA-138 in GBM tumorigenicity, suggesting a potential application in GBM therapy.



## 1. Introduction

Glioblastoma multiforme (GBM), with characteristics of high proliferation and infiltrative invasion, is the most common and aggressive form of malignant brain tumors, associated with poor prognosis [1,2]. However, the mechanism and effective therapies for malignant GBM remain elusive. MicroRNAs (miRNAs or miRs) are a family of endogenous small non-coding RNAs that play key roles in post-transcriptional gene regulation through targeting protein-encoding mRNAs [3,4]. Many miRNAs have been confirmed to be aberrantly deregulated in diverse human cancers and therefore involved in tumorigenesis [4]. During tumor development and progression, down-regulated miRNAs in tumors are usually recognized to act as tumor suppressors, whereas up-regulated miRNAs in tumors exert functions as oncogenes [5,6].

Accumulated evidences demonstrate that a pool of miRNAs is as well involved in gliomagenesis through modulating their target genes implicated in multiple biological processes, including cell proliferation, cell cycle, apoptosis, invasion and migration. For example, the down-regulated miR-7 is first to show to inhibit glioblastoma cell proliferation and migration by directly targeting EGFR, IRS1/2 [7] and Raf1 [8]. Another reduced miRNA in glioma, miR-326, is found to not only promote glioblastoma cell apoptosis and suppress glioma cell tumorigenicity *in vivo* by modulating Notch1/2 [9] but also reduce glioblastoma and glioma stem cell growth, cellular invasion, metabolic activity by inhibition of PKM2 [10]. Likewise, knockdown of up-regulated miRNA in glioblastoma is also beneficial for tumor control. MiR-10b is augmented in glioblastoma, and interference of miR-10b induces glioma cell cycle arrest and apoptosis, which is obtained from increase of target genes CDKN1A, CDKN2A and Bim [11]. All these studies suggest a potential future of miRNAs in glioblastoma therapy. Although tumor suppressive roles of multiple miRNAs have been observed in glioblastoma, however, efficacy of tumor inhibition is probably different among miRNAs, which receive less attention. As a result, we attempt to define the tumor suppressive miRNAs not only down-regulated in

* Corresponding author at: Department of Neurology, The Sun Yat-sen Memorial Hospital, Sun Yat-sen University, No. 107, West Yanjiang Road, Guangzhou 510120, China. Tel.: +86 20 81332595; fax: +86 20 81332833.
*E-mail address:* docpengy@yahoo.com.cn (Y. Peng).
[1] Qiu S and Huang D contributed equally to this work.

0925-4439 
http://dx.doi.org/10.1016/j.bbadis.2013.05.015

glioblastoma but also potent to inhibit expression levels of the oncogene, enhancer of zeste homolog 2 (EZH2), which has been validated to extensively participate in gliomagenesis [12–14].

EZH2 possesses the histone methyltransferase activity and can lead to gene silence through methylating histones [15,16]. EZH2 is over-abundant in a broad range of human malignancies including GBM, and contributes to tumor proliferation and cell cycle control [12,16,17]. The Cyclin-dependent kinase 4 and 6 (CDK4/6) are critical regulators of cell cycle G1/S transition and are specialized to phosphorylate and inactivate the cell cycle controller Retinoblastoma protein (Rb) [18]. Inactivation of Rb (phosphorylated Rb) in cancer cells results in the deregulation of the transcription factor E2F1, which controls the expression of genes involved in cell cycle and proliferation [19]. Actually, alternation of the CDK4/6-pRb-E2F1 pathway has been identified in the majority of human malignancies including GBM [19,20]. However, whether knockdown of oncoprotein EZH2 could trigger inactivation of CDK4/6-pRb-E2F1 pathway subsequently affecting GBM tumorigenicity remains unknown. Additionally, it is exhibited that the transcription factor E2F1 is able to drive EZH2 transcription [21]. Therefore, we come to the hypothesis that an EZH2-mediated signal loop, EZH2-CDK4/6-pRb-E2F1 is involved in gliomagenesis, and this signal loop could be suppressed by the candidate miRNA.

Here, we find out that miR-138 is the miRNA that is reduced in GBM samples and potent to inhibit EZH2 expression. Moreover, high levels of miR-138 are associated with extended survival of GBM patients. Functionally, over-expression of miR-138 is able to effectively inhibit glioblastoma tumor growth through directly targeting EZH2, CDK6, E2F2 and E2F3. Importantly, the tumor suppressive potency of miR-138 is obtained by inhibition of a potential EZH2-CDK4/6-pRb–E2F1 signal loop.

## 2. Materials and methods

### 2.1. GBM specimens

Fresh tumor specimens from 25 patients with GBM and non-neoplastic brains (NNBs) tissues from 14 patients without glioma were collected in the Department of Neurosurgery, Sun Yat-sen Memorial Hospital of Sun Yat-sen University. All the GBM tissues have been pathologically confirmed. Collected tissues for RNA detecting were immediately snap-frozen in liquid nitrogen and stored at −80 °C, while tissues for immunohistochemistry were fixed in 10% formalin and embedded in paraffin. The study was approved by our institutes' ethical committee and all patients gave informed consent.

### 2.2. TCGA dataset and patient information

MiRNA-138 and corresponding gene expression dataset and the corresponding clinical data for glioblastoma samples were downloaded from The Cancer Genome Atlas (TCGA) data portal (https://tcga-data.nci.nih.gov/tcga/tcgaHome2.jsp) and analyzed as described in Supplementary material.

### 2.3. Cell lines and culture

The normal human astrocytes (NHA) were purchased from ScienCell Research Laboratories and cultured according to the manufacturer's instructions. The human GBM cell lines U87MG, U251MG, A172, T98G, U118 and SHG-44 were obtained from China Academia Sinica cell repository, Shanghai, China. All cell lines were cultured in Dulbecco's modified Eagle's medium (Invitrogen) supplemented with 10% fetal bovine serum (Invitrogen) in a humidified atmosphere containing 5% $CO_2$ at 37 °C without antibiotics.

### 2.4. Plasmid construction and miRNA/siRNA transfection

Details of plasmid construction (primers were provided in Supplementary Table 1) and miRNA/siRNA transfection were described in Supplementary material.

### 2.5. Cell viability and EdU incorporation assays

Cell viability and EdU incorporation assays were performed according to the manufacturer' protocol, as described in Supplementary material.

### 2.6. In vivo tumorigenicity assay

Female BALB/c nude mice aged 4–5 weeks were purchased from Laboratory Animal Center of the Sun Yat-sen University. All animal experimental procedures were performed under the approval of the Institutional Animal Care and Use Committee of the Sun Yat-sen University. Two nude mouse models of GBM xenograft tumors were established and details were described in Supplementary material.

### 2.7. Cell cycle analysis

Cell cycle distribution analysis was performed by flow cytometry (FCM; BD) as described in Supplementary material.

### 2.8. Dual luciferase reporter assays

For dual luciferase reporter assays, miRNAs and EZH2/CDK6/E2F2/E2F3 wild/mutant 3′-UTR plasmids were co-transfected in U87 cells for 48 h and then luciferase assays were performed using the dual-luciferase reporter Assay system (Promega) according to the manufacturer's instructions. All experiments were repeated at least three times with duplicate samples.

### 2.9. RNA extraction and quantitative real-time PCR

Total RNA and quantitative real-time PCR (qPCR) was performed according to conventional protocol and as described in Supplementary material (primers were provided in Supplementary Table 1).

### 2.10. Immunohistochemistry and Western blotting

Immunohistochemistry (IHC) and Western blot analysis were carried out according to conventional protocol and as described in Supplementary material.

### 2.11. Statistical analysis

Quantitative data were expressed as mean ± SEM. Statistical analysis was performed with the SPSS13.0 software (version 13.0; SPSS Inc.) using two-tailed Student's *t* test or one-way analysis of variance for experiments with more than two subgroups. Survival analysis was carried out with the Kaplan–Meier method and the survival curve was generated by GraphPad Prism (version 5.04; GraphPad Software, Inc.). Correlation analysis was made by using two-tailed Pearson correlation coefficient. $p < 0.05$ was considered statistically significant.

## 3. Results

### 3.1. MiR-138 was potent to target EZH2 mRNA in human glioblastoma

Given the importance of EZH2 in GBM progression, we tried to identify a down-regulated miRNA in glioblastoma acting as a tumor

suppressor to effectively target the oncogene, EZH2. Initially, using miRanda, PICTAR5, miRWalk and TargetScan, we predicted 231 miRNAs targeting EZH2 3′-UTR (Supplementary Table 2). Then, we reviewed 60 down-regulated miRNAs in GBM according to microarray data in publications (Supplementary Table 3). Next, we integrated the lists of miRNAs in two supplementary tables and produced a new list of 13 miRNAs that were not only predicted to target EZH2 but also were confirmed down-regulated in GBM (Supplementary Table 3). Finally, using luciferase activity assays, miR-98, miR-101, miR-137, miR-138 and miR-323 were shown to decrease luciferase activities by almost 50% relative to NC. Notably, miR-138 reduced the luciferase activity to 34.5% compared with NC, indicating a strong potency of miR-138 on inhibiting EZH2 expression in GBM (Fig. 1A).

### *3.2. Expression levels of miR-138 were reduced in human GBM and were associated with survival of GBM patients*

Then, expression levels of miR-138 were assessed both in GBM cell lines and clinical samples. Initially, real-time qPCR analysis confirmed that expression levels of miR-138 were significantly reduced in all GBM cell lines compared to NNB samples (Fig. 1B). Secondly, expression levels of miR-138 in 25 GBM and 14 NNB specimens were analyzed,

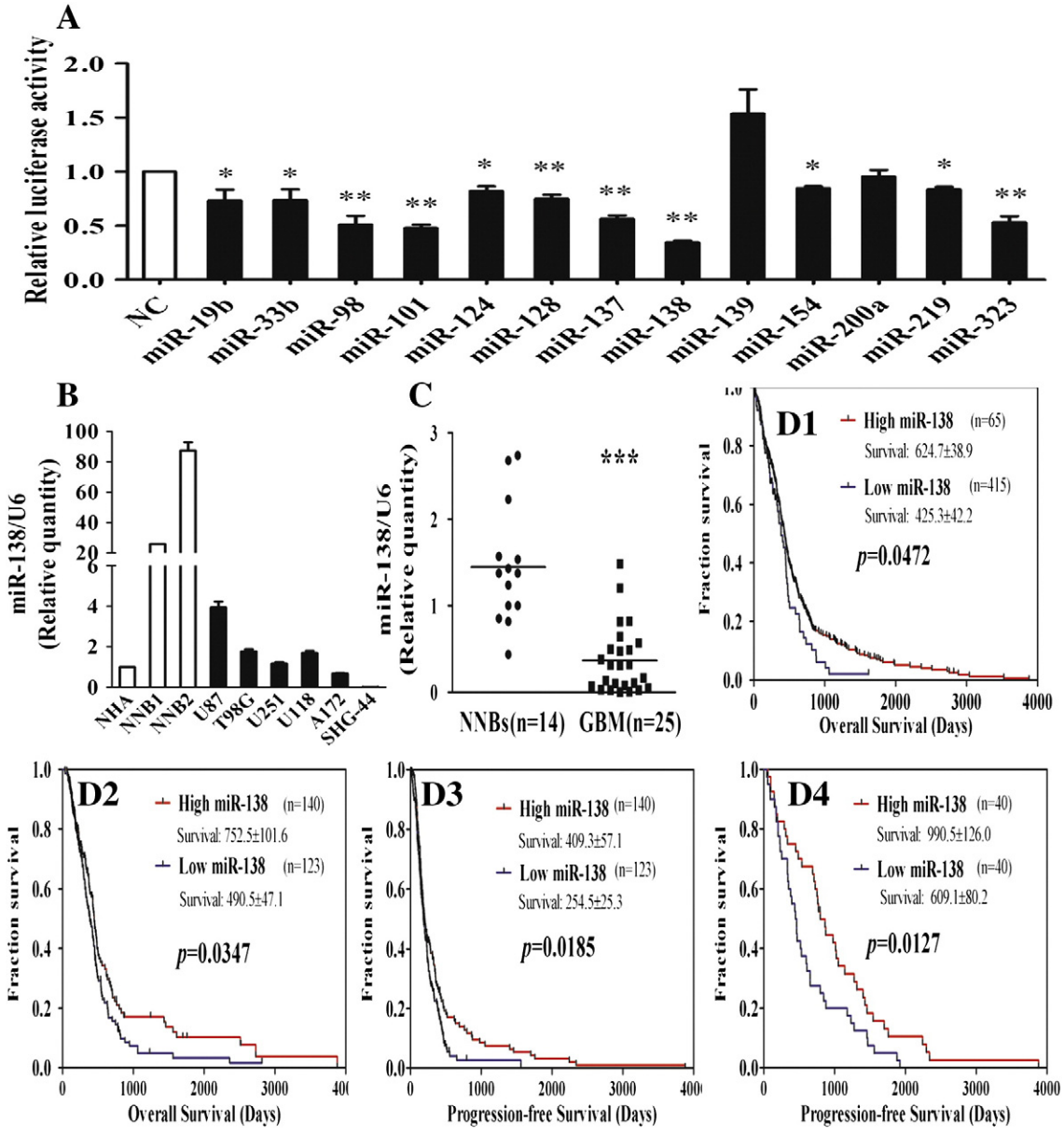


**Fig. 1.** MiR-138 was potent to target 3′-UTR of EZH2 mRNA and reduced in GBM cell lines and specimens. A. Mimics of miRNAs that were down-regulated in glioma and predicted to target EZH2 3′-UTR were co-transfected with psiCHECK2-EZH2 3′-UTR plasmids into U87 glioma cells for 48 h, and then their interactions were determined by dual luciferase reporter analysis. Data was a summary of 2 independent experiments and each was performed in triplicate. B. Expression of miR-138 determined by stem-loop q PCR was reduced in GBM cell lines U87, U251 and A172, T98G, U118 and SHG-44. The NHA cell line and two human NNB samples were used as controls. C. Expression of miR-138 was down-regulated in GBM specimens (n = 25) compared with NNBs (n = 14) as determined by stem-loop qPCR. D. Extended OS and PFS of GBM patients from TCGA dataset were associated with high miR-138 expression at different stratifications. D1: High miR-138 was related with long OS among the whole TCGA dataset at the indicated cut-off. D2 and D3: High levels of miR-138 were associated with longer OS and PFS from a 263 patient dataset. D4: At the stratification of patient survival longer than 2 years, high levels of miR-138 significantly correlated with extended PFS of GBM patients. The Log-rank test p value for the difference between two survival curves for the miR-138-high and -low expression GBM patients was indicated. *, $p < 0.05$ vs NC; **, $p < 0.01$ vs NC; ***, $p < 0.001$ vs NNBs.

and obvious down-regulation of miR-138 in GBM samples was also demonstrated (Fig. 1C). Moreover, using the TCGA data including 480 GBM samples and 10 normal tissues, we obtained the same trend that expression of miR-138 was significantly decreased in GBM samples in comparison to NNB samples (6.80 ± 0.76 vs 8.73 ± 0.39, Supplementary Fig. 1). These results suggested that miR-138 was correlated with GBM tumorigenesis.

Also, using TCGA clinical information dataset with qualified patients, we performed overall survival (OS) and progression-free survival (PFS) analysis of GBM patients. Using the whole clinical dataset with 480 patients accompanied by qualified miR-138 expression, we only found that high level of miR-138 was associated with long OS relative to low level of miR-138 at the stratification of n = 65 (high miR-138) as the cut-off (mean survival: 624.7 ± 38.9 vs 425.3 ± 42.2 days; p = 0.0472; Fig. 1D1), although other possible stratification conditions had been tested. Then, Kaplan–Meier analysis of 263 patients without surgery also showed that patients with high miR-138 levels were related with longer OS compared with low levels of miR-138 (mean survival: 752.5 ± 101.6 vs 490.5 ± 47.1 days; p = 0.0347; Fig. 1D2), and that, likewise, high miR-138 levels were correlated with more extended PFS in comparison to low miR-138 levels (409.3 ± 57.1 vs 254.4 ± 25.3 days; p = 0.0185; Fig. 1D3). Moreover, at the stratification of patient survival longer than 2 years, high levels of miR-138 significantly extended PFS of GBM patients in relative to low levels of miR-138 (mean survival: 990.5 ± 126.0 vs 609.1 ± 80.2 days; p = 0.0127; Fig. 1D4). Both expression and survival analysis of miR-138 suggested that miR-138 was associated with in GBM tumor biology.

### 3.3. MiR-138 suppressed GBM cell proliferation and induced cell cycle arrest in vitro

Next, the impact of miR-138 on GBM cell proliferation was investigated. First, MTT assays showed that over-expression of miR-138 in U87 and U251 cells reduced tumor cell viabilities to approximately maximal 30% relative to NC treatments (Fig. 2A). Then, cell proliferation was further evaluated by EdU incorporation assays and the results illustrated that, compared with NC, miR-138 obviously decreased cell proliferation with approximately 50% reduction of ratios of EdU positive cells in both U87 and U251 cells (Fig. 2B and C).

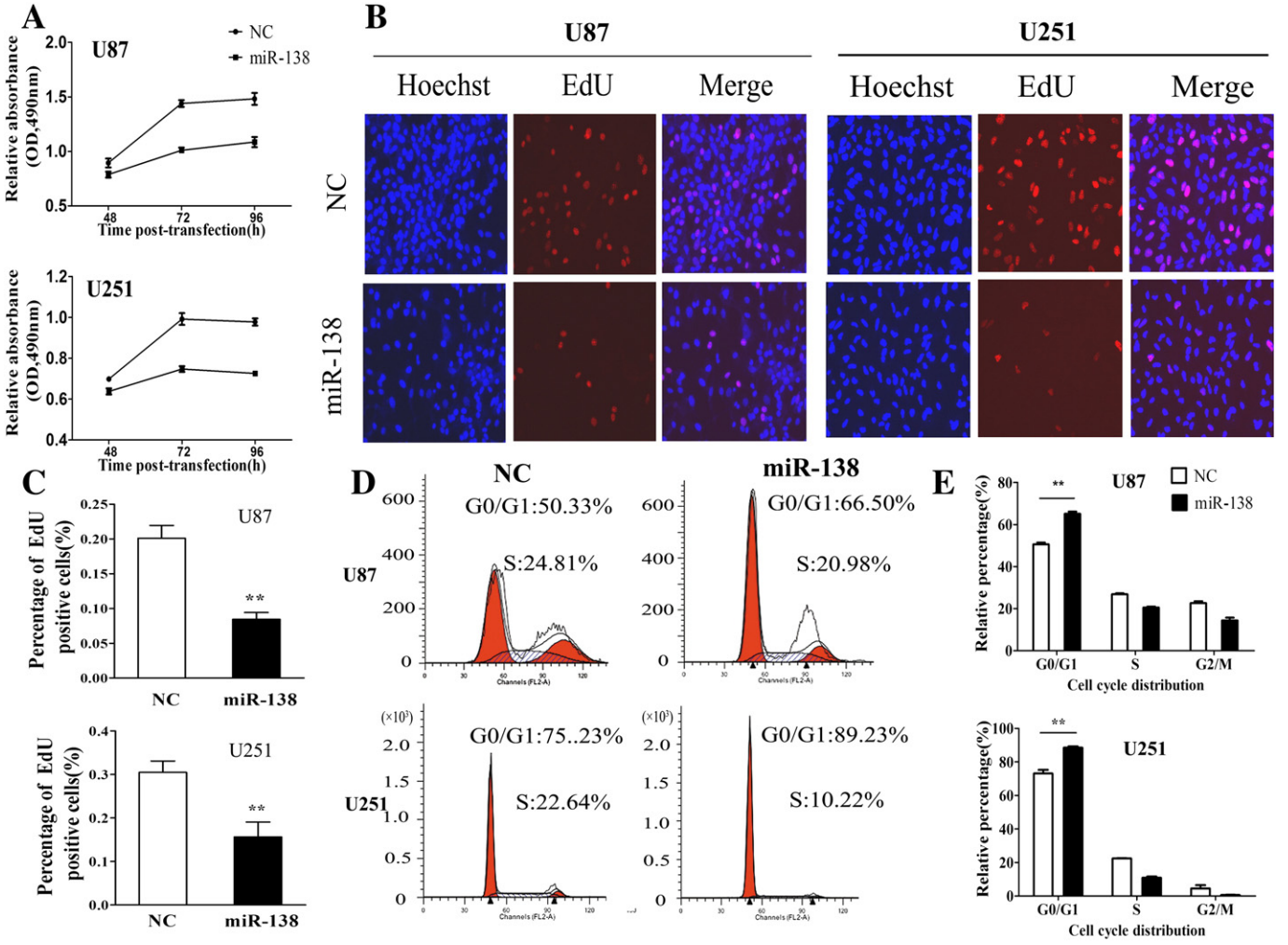


**Fig. 2.** MiR-138 suppressed GBM cell viability and proliferation and induced cell cycle arrest *in vitro*. A. Glioma cell viability was measured by MTT assay in U87 and U251 cells 48, 72 or 96 h after miR-138 or negative control (NC) transfection. B and C. Glioma cell proliferation was displayed by EdU analysis in U87 (left panel) and U251 (right panel) cells 72 h after miR-138 or NC transfection (B). The percentage of EdU positive cells was defined as the ratio of EdU positive cells to total Hoechst positive cells. The EdU positive cells (red) and Hoechst-staining cells (blue) were counted in five visual fields at 200× magnification. D and E. Cell cycle distributions were performed by FCM in U87 and U251 cells 72 h after miR-138 or NC transfection. Graphical representation of the cell cycle distributions from one experiment (D). Statistic analysis of cell cycle distributions from three repeating experiments (E). **, p < 0.01 vs NC.

To investigate the potential mechanism by which miR-138 suppressed GBM cell proliferation, we evaluated cell cycle distributions using the FCM analysis. After 72 h transfection, both U87 and U251 cells transfected with miR-138 distributed cell cycle arrest of G1/S progression, with approximately 15% elevation of G1 phase proportion in U87 cells and 16% of U251 cells compared to NC-transfected cells (Fig. 2D and E). This result implied that miR-138 suppressed GBM cell proliferation through blocking G1/S transition of cell cycles.

### 3.4. MiR-138 suppressed tumor growth of GBM cells in nude mice

Then, two *in vivo* models were employed to investigate the suppression of miR-138 on GBM tumor growth. First is the pretreated xenograft model. U87 cells pre-treated with agomir-138 were injected subcutaneously into nude mice. Tumor sizes were measured every 2 days. When tumors size reached the volume of 1000 $mm^3$, mice were sacrificed and tumors were dissected and weighed. After two weeks of injection, tumors of agomir-NC pretreated group grew much larger and faster than agomir-138 pretreated group (Fig. 3A). At the endpoint, the tumor volume of agomir-138 group was significantly smaller than that of agomir-NC group (479.88 ± 150.75 vs 1084.11 ± 264.10 $mm^3$), while the tumor weight of agomir-138 group was almost reduced to half of agomir-NC group (Fig. 3B, C and D). Moreover, as an indicator of cell proliferation, Ki-67 staining from an agomir-NC xenograft was more frequent and stronger than that of agomir-138 treated model (Fig. 3E).

To further confirm this *in vivo* suppression and assess feasibility of using miR-138 therapeutics for malignant glioma treatment, the intratumoral injection model was constructed. Subcutaneous xenograft tumors were first produced with U87 cells, then cut up into the same square blocks of approximately 2 $mm^3$ and transplanted into nude mice. After 9-day incubation, agomir-138 was directly injected into xenograft tumor models. Even though intratumoral injections could not achieve uniform spread of miRNA in tumors, agomir-138 remarkably suppressed the growth of xenografts as illustrated by reductions of tumor sizes and weight. After approximately 2-week injection, both tumor volume and weight of agomir-NC group were twice that of agomir-138 group (Fig. 3F, G and H).

### 3.5. EZH2, CDK6, E2F2 and E2F3 were direct targets of miR-138 in GBM cells

To find out the mechanisms by which miR-138 inhibited gliomagenesis, we predicted the potential targets of miR-138 using TargetScan and PicTar algorithms, and EZH2, CDK6, E2F2 and E2F3 were predicted as putative targets of miR-138. Luciferase reporter vectors containing wild type (mt) and mutant type (mut) 3′-UTR sequences of EZH2, CDK6, E2F2 and E2F3 were constructed (Fig. 4A). U87 cells were co-transfected with EZH2, CDK6, E2F2, or E2F3 mt or mut 3′-UTR vectors and miR-138 mimics for 48 h. Compared with NC, co-transfection of miR-138 and EZH2 wt 3′-UTR plasmids resulted in significant decrease in luciferase activity approximately by 65%, with mut1 and mut2 by about 20% and 35% respectively, while mut1 + 2 almost did not reduce luciferase activity (Fig. 4B). This result suggested that miR-138 directly targeted both binding sites within the EZH2 3′-UTR, and that two miR-138 recognition sites of EZH2 3′-UTR exerted an additive action. Likewise, co-transfection of miR-138 and CDK6, E2F2 or

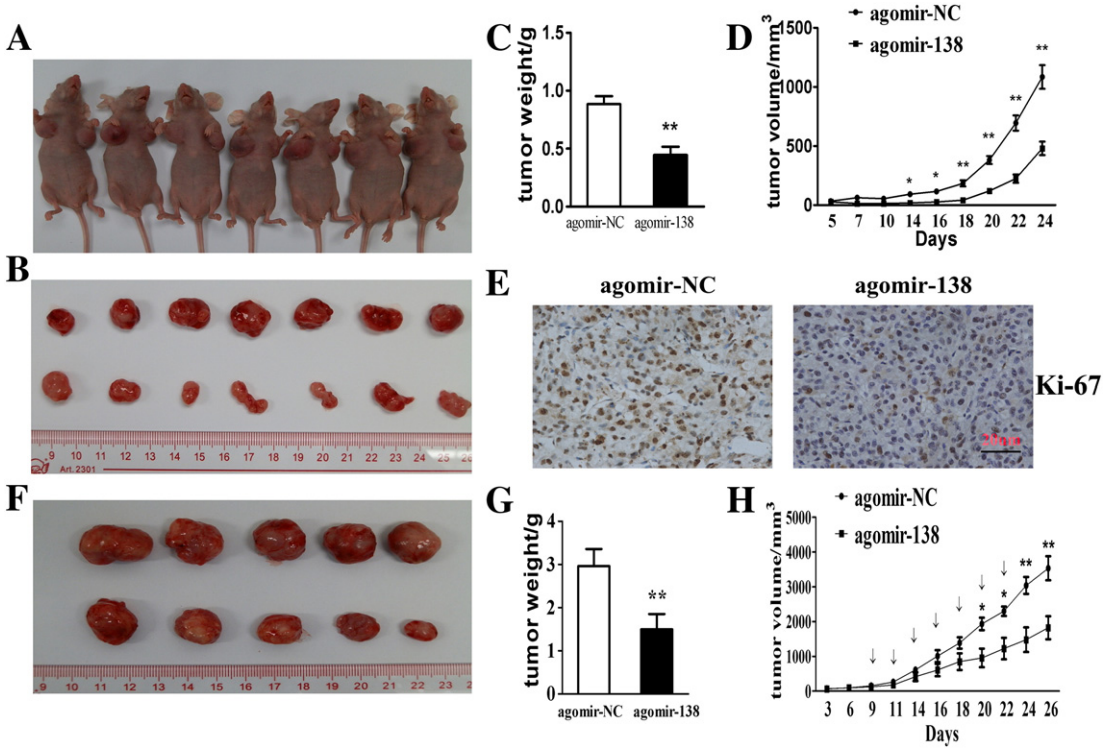


**Fig. 3.** MiR-138 suppressed tumor growth of GBM cells in nude mice. A and B. U87 cells pre-treated with agomir-NC or agomir-138 were injected subcutaneously into the right or left armpit of the same nude mice. Tumor sizes were measured every 2 days. When tumors size reached the volume of 1000 $mm^3$, mice were sacrificed and tumors were dissected and weighed. The mice and tumor were exhibited (A and B). C. Comparing of tumor weights from agomir-138 and agomir-NC pretreated groups (n = 7). D. Growth curve of tumor volumes from the same group as C. Each data point represents the mean ± SEM of 7 tumors. E. Examination of levels of Ki-67 by IHC in slice samples from pretreated injection models (×400 magnification). F. Agomir-138 suppressed tumor growth in intratumoral injection model. Subcutaneous xenograft tumors were first produced with U87 cells, then cut up into the same square blocks of approximately 2 $mm^3$ and transplanted into right flanks of nude mice. After 9-day incubation, agomir-138 and agomir-NC were directly injected into xenograft tumor models. Arrows indicated the injection time points. G. Comparing of tumor weights from intratumoral models (n = 5). H. Growth curve of tumor volumes. Each data point represents the mean ± SEM of 5 tumors from intratumoral model. *, $p < 0.05$ vs NC; **, $p < 0.01$ vs NC.

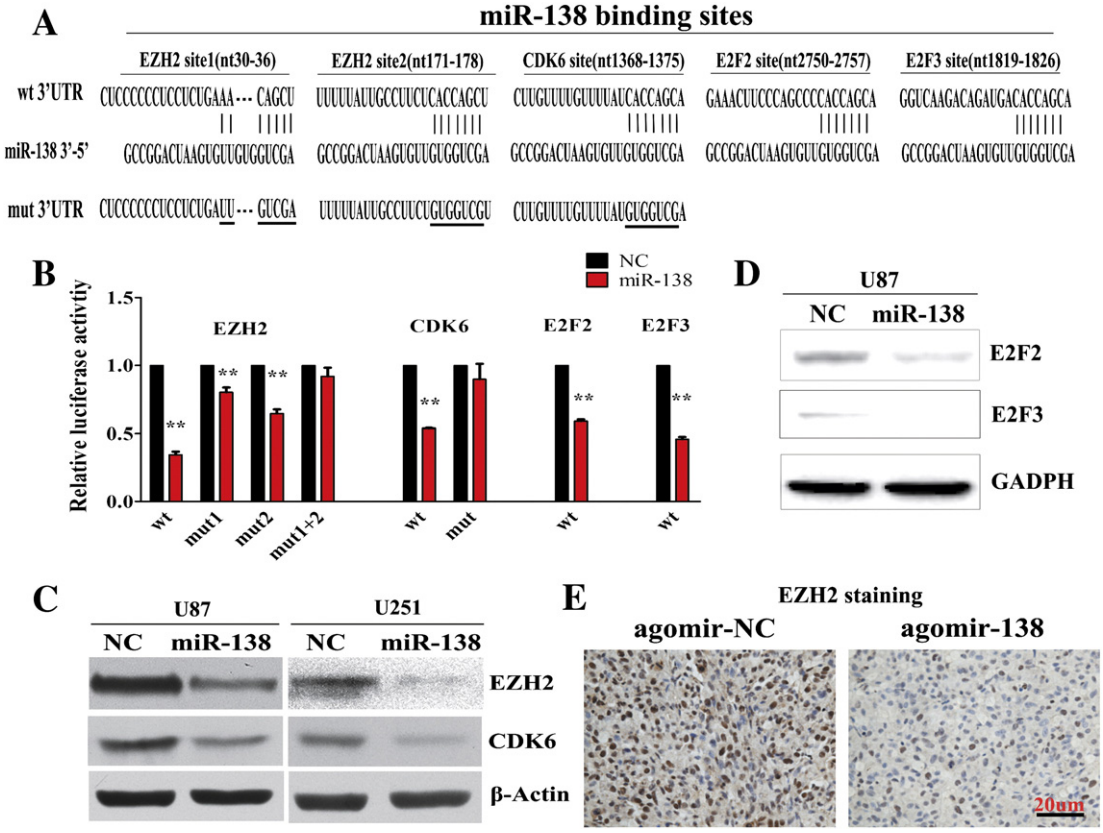


**Fig. 4.** EZH2, CDK6, E2F2 and E2F3 were direct targets of miR-138. A. The potential interactions between miR-138 and putative binding sites in 3′-UTRs of EZH2, CDK6, E2F2 and E2F3 were predicted by PicTar or TargetScan algorisms. Complementarities between miR-138 'seed sequence' and wild-type (wt) 3′-UTRs of putative target genes were exhibited. Mutant type 1 (mut1) of EZH2 was mutant at binding site 1, mut2 was mutant at binding site 2, and mut1 + 2 were mutant at both binding sites. B. Luciferase activities were evaluated in U87 cells 48 h after co-transfection of miR-138 mimics and wt or mut 3′-UTR vectors of target genes, with the final concentrations of 100 nM for miR-138 mimic and 10 ng/μl for target genes 3′-UTR vectors. Data were presented as a summary of two separate experiments performed in triplicate. C. Expression of EZH2 and CDK6 protein was determined by Western blot in U87 and U251 cells 72 h after transfection of miR-138 or NC. β-Actin was used as a loading control. D. Expression of E2F2 and E2F3 was determined by Western blot in U87 cells 72 h after transfection of miR-138 or NC. GAPDH was used as a loading control. E. Examination of levels of EZH2 by IHC in tumor slice samples from pretreated injection model (×400 magnification). **, $p < 0.01$ vs NC.

E2F3 wt 3′-UTR showed significant reductions of luciferase activities approximately by 50% compared with NC, whereas CDK6 mut 3′-UTR was unaffected by simultaneous transfection with miR-138 (Fig. 4B). Then, the inhibitory impact of miR-138 on EZH2, CDK6, E2F2 and E2F3 was verified at protein levels both *in vitro* and *in vivo*. Immunoblot assays confirmed that ectopic expression of miR-138 obviously inhibited expression levels of EZH2, CDK6, E2F2 and E2F3 in U87 or U251 cells (Fig. 4C and D). In addition, using tumor tissues from pretreated xenograft models, EZH2 staining in agomir-138 treated tumor tissues was weaker and less frequent than that of agomir-NC by the IHC assay (Fig. 4E). These data indicated that EZH2, CDK6, E2F2 and E2F3 were authentic targets of miR-138 in GBM cells.

### *3.6. EZH2 and CDK6 rescued the function of miR-138 in GBM cells*

Because miR-138 was not correlated with E2F2 and E2F3 (see below 3.8), we performed function-rescuing experiments only associated with EZH2 and CDK6 to assess whether the tumor suppressor effect of miR-138 was mediated by repression of EZH2 and CDK6 in GBM cells. Cells were co-transfected with expression plasmids of EZH2 or CDK6 and miR-138 mimics for 72 h. For convenience, we just performed one assay to evaluate cell proliferation for each rescuing experiment. Using MTT assays, EZH2 over-expression was shown to restore cell viabilities inhibited by miR-138 (Fig. 5A), while over-expression of CDK6 could restore cell proliferation as inhibited by miR-138 with EdU incorporation assays (Fig. 5C and D). Meanwhile, consistent with these functional studies, protein levels of EZH2 and CDK6 inhibited by miR-138 could be recovered by forced expression of EZH2 or CDK6 (Fig. 5B and E). Collectively, these data suggested that EZH2 and CDK6 mediated the tumor suppressive role of miR-138 in glioblastoma cells. In other words, EZH2 and CDK6 were functional targets of miR-138.

### *3.7. MiR-138 inhibited the EZH2-CDK4/6-pRb-E2F1 signal loop in GBM cells*

As we know, CDK4/6-pRb-E2F1 pathway is critical for cell cycle control of G1/S transition [22]. Based on our observations of glioblastoma cell cycle G1/S arrest and EZH2 inhibition by miR-138, we hypothesized that miR-138 repressed tumor proliferation through inhibiting EZH2-mediated CDK4/6-pRb-E2F1 pathway.

First, using TCGA gene data, we evaluated relationship between EZH2 and molecules that were linked with G1/S progression. Pearson's correlation analysis showed that, in GBM samples, expression levels of EZH2 were positively and strongly correlated with E2F1 and E2F3 levels, and were marginally associated with CDK4 and CDK6 levels with $r^2 = 0.418$ and 0.322 for E2F1 and E2F3, respectively (Fig. 6A), whereas EZH2 levels were marginally negatively related with E2F2 levels (Supplementary Fig. 2) Likewise, EZH2 levels also exhibited positive associations with other cell cycle-promoting molecules related

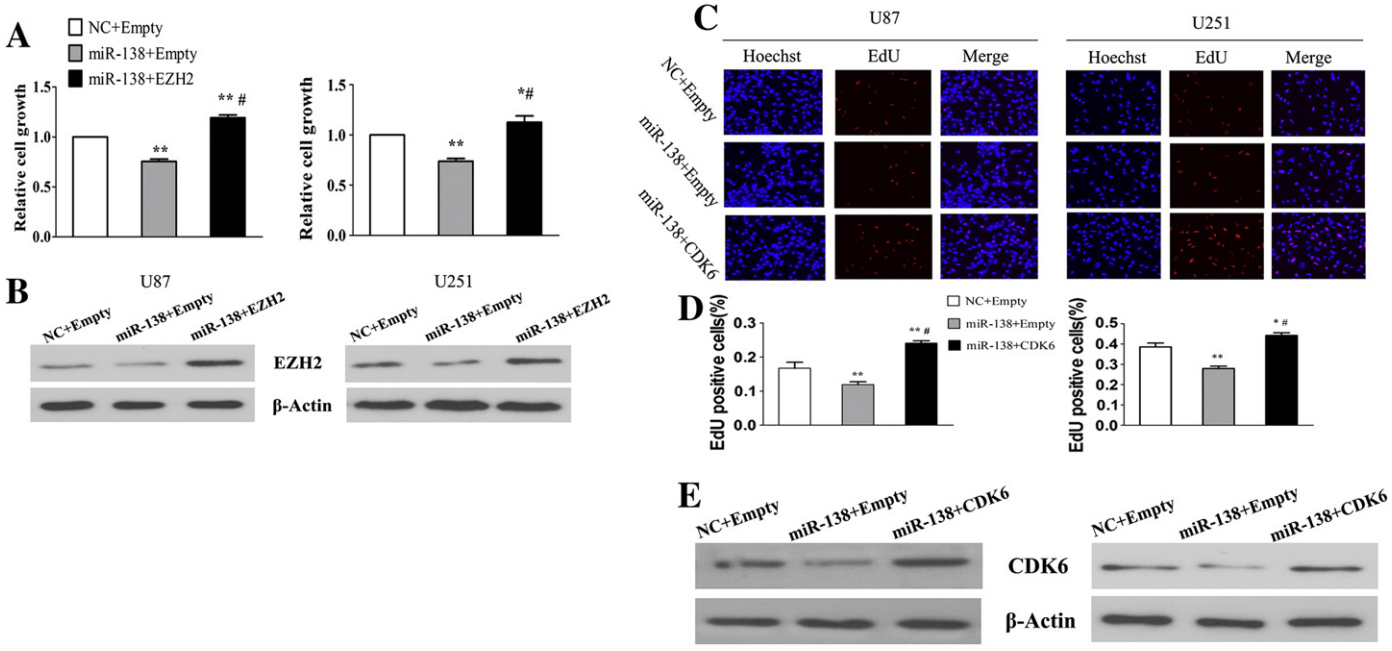


**Fig. 5.** EZH2 and CDK6 rescued the function of miR-138 in GBM. A. U87 or U251 cells were co-transfected with miR-138 mimic and EZH2 expression plasmids for 72 h. And then cell viabilities were determined by MTT assay. B. Similar co-transfection as A. Expression of EZH2 protein was analyzed by Western blot. C. U87 or U251 cells were co-transfected with miR-138 mimic and CDK6 expression plasmids for 72 h. Then, cell proliferation was determined by EdU assay. D. Graphic representation of percentage of EdU positive cells in C. E. Similar co-transfection as C. Expression of CDK6 protein was analyzed by Western blot. *, $p < 0.05$ vs NC + empty; **, $p < 0.01$ vs NC + empty; #, $p < 0.01$ vs miR-138 + empty.

with G1/S, such as CCND1, CCND2, CCNE1 and CCNE2, with $r^2 = 0.289$ and $r^2 = 0.480$ for CCNE1 and CCNE2, respectively (Supplementary Fig. 2). Moreover, EZH2 was negatively associated with the cell cycle inhibitor CDKN1A in GBM samples, even though other cell cycle inhibitors RB1, P53 and CDKN2A were marginally positively related with EZH2 levels (Supplementary Fig. 2). These results of correlation

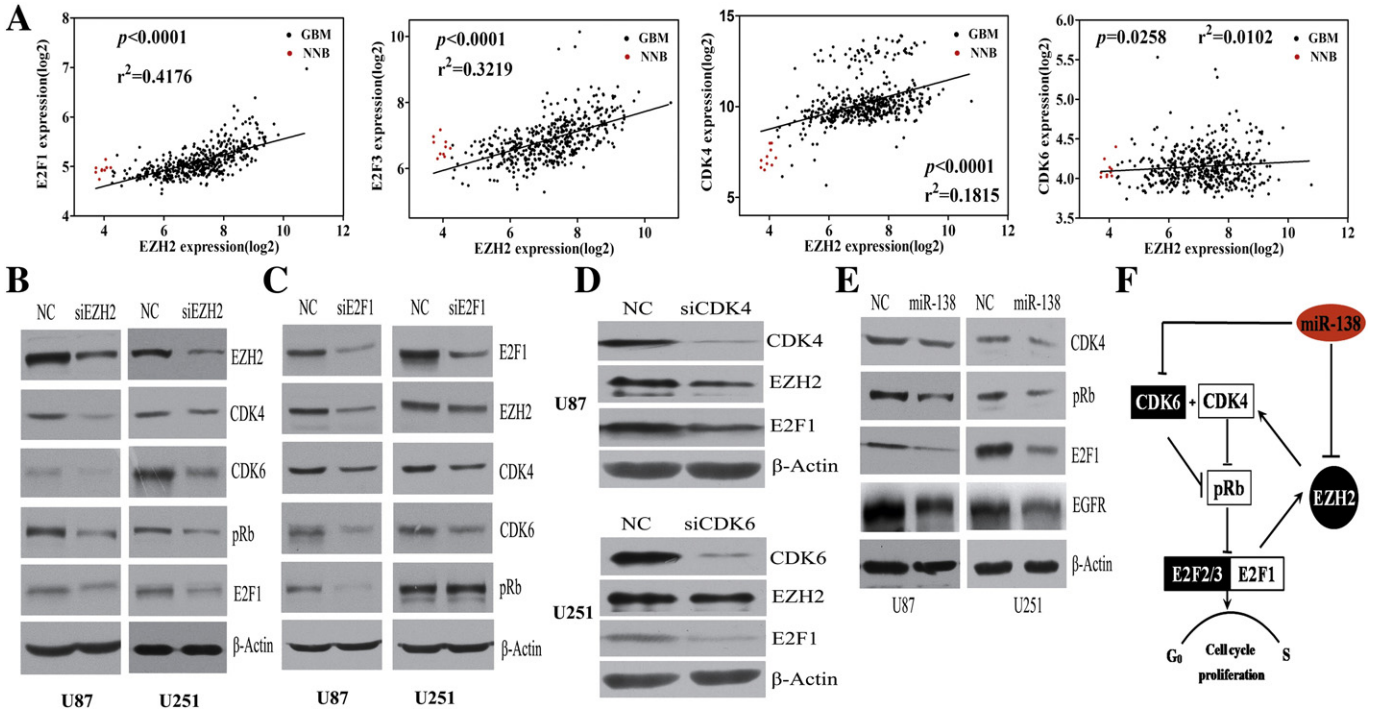


**Fig. 6.** MiR-138 inhibited the EZH2-CDK4/6-pRb-E2F1 signal loop in GBM cells. A. Using TCGA gene expression data, relationship between EZH2 and E2F1, E2F3, CDK4 and CDK6 was performed by Pearson's correlation analysis. B. U87 and U251 cells were transfected with siEZH2 for 48 h and then expression levels of EZH2, E2F1, CDK4, CDK6 and pRb were determined by Western blot. β-Actin was used as a loading control. C. U87 and U251 cells were transfected with siE2F1 for 48 h and then expression levels of E2F1, EZH2, CDK4, CDK6 and pRb were determined by Western blot. β-Actin was used as a loading control. D. U87 cells were transfected with siCDK4 for 48 h and then expression levels of CDK4, EZH2, E2F1 were determined by Western blot (upper). U251 cells were transfected with siCDK6 for 48 h and then expression of CDK6, EZH2 and E2F1 were determined by Western blot (lower). E. Expression levels of CDK4, pRb, E2F1 and EGFR were determined by Western blot after 72 h transfection of miR-138 mimics to U87 or U251 cells. F. A diagram of EZH2 mediated signal loop which could be blocked by miR-138 in GBM cells. Black box denotes targets of miR-138.

analysis strongly suggested that EZH2 was thoroughly and extensively implicated in glioblastoma cell cycle control.

Subsequently, regulation of EZH2 on expression of cell cycle G1/S related molecules, such as CDK4, CDK6, pRb and E2F1-3, was evaluated in glioblastoma cell lines, and the immunoblot assay showed that expression levels of CDK4, CDK6, pRb and E2F1-3 were significantly reduced after knockdown of EZH2 with effective siEZH2, compared with NC-transfected cells (Fig. 6B and Supplementary Fig. 3). Together with correlation analysis above, these *in vitro* results indicated that EZH2 took part in cell cycle control and proliferation though modulating cell cycle related proteins.

Interestingly, it was reported that E2F1 directly bound to EZH2 promoter to drive its transcription [21]. Therefore, we hypothesized that an EZH2-CDK4/6-pRb-E2F1 signal loop probably existed in GBM mediating tumor proliferation and cell cycle. To test this idea, we transfected both U87 and U251 cells with effective siE2F1 due to the importance of E2F1 other than E2F2 and E2F3, and found that knockdown of E2F1 induced significant reduction of EZH2, CDK4, CDK6 and pRb proteins (Fig. 6C). To further verify the existence of this signal loop, cells were treated with effective siRNAs of CDK4 or CDK6, and then notable reduction of EZH2 and E2F1 protein was observed, although knockdown of CDK6 did not show a significant decrease of EZH2 expression (Fig. 6D). Together, our data suggested that an EZH2-CDK4/6-pRb-E2F1 signal loop existed in glioblastoma mediating cell cycle and proliferation.

However, CDK4, pRb and E2F1 were predicted not as putative targets of miR-138, and thus, regulations of miR-138 on these proteins needed to be assessed. Compared with NC-treated cells, U87 and U251 cells-transfected with miR-138 showed remarkable down-regulation of CDK4, pRb and E2F1 proteins (Fig. 6E). Notably, Epidermal Growth Factor Receptor (EGFR) is considered as one biomarker for glioblastoma, and moreover, it is involved in cell cycle control and proliferation of glioma [23]. As a result, expression of EGFR was determined in miR-138 treated glioblastoma cells, and significant down-regulation of EGFR was observed, which further strengthened the inhibitory role of miR-138 in GBM cell proliferation (Fig. 6E).

Collectively, these results strongly suggested that an EZH2-CDK4/6-pRb-E2F1 signal loop existed in glioblastoma cell proliferation and cell cycle control, which could be suppressed by miR-138, leading to tumor growth inhibition (Fig. 6F).

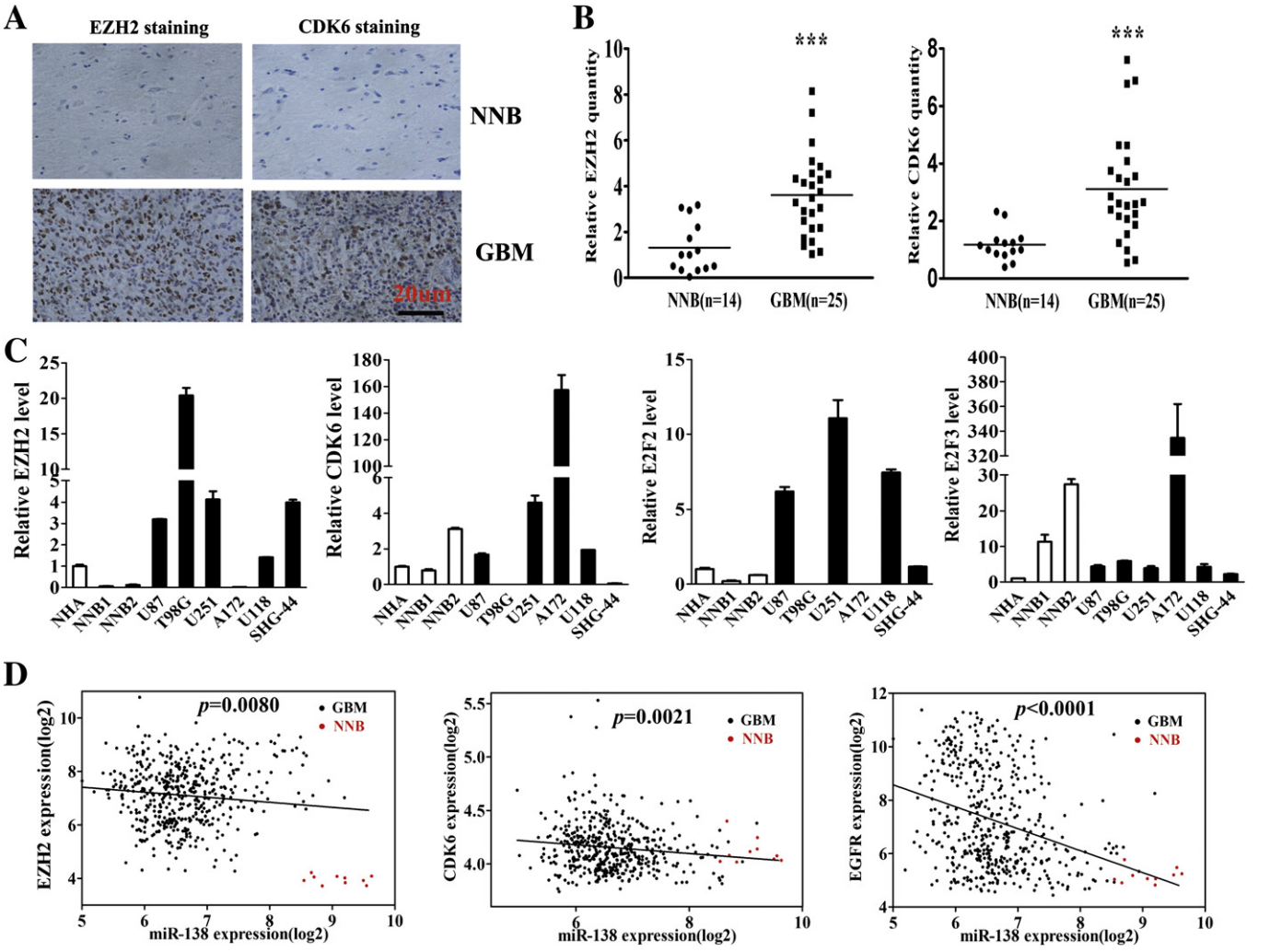


**Fig. 7.** Correlation analysis between miR-138 and target genes in GBM clinical samples. A. IHC displayed more frequent and stronger nuclear staining of EZH2 and CDK6 positive cells in GBM tissues than NNB samples at the magnification of 400×. B. Expression levels of EZH2 and CDK6 were determined by q-PCR in GBM and NNB samples. C. Expression levels of EZH2, CDK6, E2F2 and E2F3 were determined by q-PCR in GBM cell lines. NHA and two NNB samples were used as controls. D. Two-tailed Pearson's correlation analysis reported that miR-138 levels were inversely correlated with EZH2, CDK6 and EGFR mRNA expression in 480 GBM and 10 NNB clinical samples from TCGA dataset. ***, $p < 0.001$ vs NNB.

### 3.8. Levels of miR-138 inversely correlated with expression levels of EZH2 and CDK6 in GBM and NNB samples

Initially, IHC displayed high frequency and strong staining of EZH2 and CDK6 positive cells in GBM specimens than NNB tissue (Fig. 7A). Next, we evaluated mRNA levels of EZH2 and CDK6 in 25 GBM specimens by q-PCR, and the results showed that both expression levels of EZH2 and CDK6 were significantly increased in GBM samples in comparison to NNB tissues (Fig. 7B). Then, relative quantity of EZH2, CDK6, E2F2 and E2F3 in NHA and GBM cell lines was analyzed by q-PCR. Compared with NHA or NNB samples, all levels of EZH2, CDK6, E2F2 and E2F3 were almost increased in GBM cell lines (Fig. 7C). Then, we sought to find out the association between EZH2, CDK6, E2F2 or E2F3 and miR-138 using TCGA dataset with 480 GBM and 10 NNB samples with two-tailed Pearson's correlation analysis, and the results showed that both levels of EZH2 and CDK6 were negatively correlated with expression of miR-138 ($p = 0.008$ and 0.002, respectively; Fig. 7D), while E2F2 and E2F3 were marginally correlated with levels of miR-138 (Supplementary Fig. 4). Meanwhile, using our small amounts of samples, we found the same trends between miR-138 levels and EZH2 or CDK6 levels ($r^2 = 0.303$ or 0.341; $p < 0.0001$; Supplementary Fig. 5). Moreover, an inverse association was also observed between miR-138 and GBM biological marker EGFR (Fig. 7D). These results further validated the inhibitory effects of miR-138 on EZH2, CDK6 and EGFR, although no negative relationship between E2F2 or E2F3 and miR-138 was observed in clinical samples.

## 4. Discussion

It is well demonstrated that deregulation of miRNAs contributes to carcinogenesis. Hence, restoring deregulated miRNAs maybe leads to tumor suppression. In our study, we showed that miR-138 was down-regulated in GBM clinical specimens and cell lines, and that over-expression of miR-138 effectively suppressed GBM cell proliferation *in vitro* and tumorigenicity *in vivo*. Furthermore, we firstly confirmed that miR-138 directly bound to 3′-UTR of CDK6, E2F2 and E2F3. More interestingly, an EZH2-CDK4/6-pRb-E2F1 signal loop was probably involved in GBM tumorigenicity and miR-138 acquired tumor inhibitory function through blocking this signal loop.

MiR-138 is involved in a pool of essential biological processes, such as modulating DNA damage response [24], keratinocyte senescence [25], regulating dendritic spine morphogenesis [26], modulating cardiac morphogenesis during embryonic development [27], and affecting thermotolerance acquisition [28]. Dysfunction of miR-138 has been observed in several types of tumors. MiR-138 not only suppresses cell migration and invasion through targeting RhoC and ROCK2 [29], but also inhibits epithelial–mesenchymal transition through targeting VIM, ZEB2 and EZH2 in tongue squamous cell carcinoma [30]. MiR-138 also inhibits expression of HIF-1a, leading to apoptosis elevation and migration reduction in clear cell renal cell carcinoma cells [31]. Moreover, miR-138 is recently shown to inhibit tumor growth and block cell cycle arrest of hepatocellular carcinoma (HCC) by targeting cyclin D3 (CCND3) [32]. Also, it is confirmed to suppress nasopharyngeal carcinoma tumorigenesis by targeting the cyclin D1 (CCND1) [33]. In addition, miR-138 also takes part in lung cancer [34,35], thyroid cancer [36] and leukemia [37]. Consistent with the tumor suppressive role of miR-138 as above, our studies showed that miR-138 effectively inhibited GBM tumor growth. However, inconsistently, miR-138 did not show significant inhibition in cell proliferation and migration of glioblastoma SF126 cell line, although apparent reduction of miR-138 has been observed [38]. This discrepancy may be due to different cell lines of study.

Recently, Chan et al.'s publication reported that miR-138 was increased in glioma stem cells (GSCs) in comparison to normal neural stem cells (NSCs), promoted growth and survival of GSCs, and was associated with GBM patient recurrence, which was suggested as prognostic biomarker for GBM patients [39]. However, several concerns should be noted. One was that GSCs account for minority of glioma cells, and it was still lacking well-performed approach to identify and isolate GSCs from glioma samples [40–42]. Second, almost all microarray and qPCR results showed that miR-138 was reduced in glioma samples, which was also indirectly confirmed by Chan et al.'s study that level of miR-138 was down-regulated after differentiation of GSC cells. Moreover, using clinical information from TCGA dataset, Chan et al.'s report showed that there was no significant association between OS and miR-138, even though high miR-138 was prone to be associated with short survival. However, our analysis demonstrated that high miR-138 correlated with extended OS and PFS at several stratification conditions. As a result, it may be more plausible that low miR-138 served as predictor for GBM patients' outcome. However, these discrepancies suggested the importance of miR-138 in GBM tumorigenesis.

EZH2 is deregulated in a wide range of cancer types, and has a crucial role in stem cell maintenance and tumor development [43]. Actually, EZH2 is essential for glioblastoma cancer stem cell maintenance [13]. Several groups showed that tumor cell proliferation and tumor growth were restricted after deletion of EZH2 expression by miR-101 [44], miR-26a [45], miR-124 and siEZH2 [33]. Although EZH2 as a target of miR-138 has been reported in one study associated with chicken thermal control [28], we firstly defined that EZH2 was a functional target of miR-138 in GBM cells and importantly, inverse correlation of between miR-138 and EZH2 was determined in GBM specimens and cell lines. Also, CDK6 was identified as a GBM oncogene critical in G1/S transition of cell cycle, and depletion of CDK6 suppressed cell proliferation and viability in GBM cell lines and intracranial xenografts [18,46]. In our study, CDK6 was firstly confirmed as a direct functional target of miR-138, which was similar to that of miR-137 and miR-124 inhibited GBM and medulloblastoma proliferation by targeting CDK6 [47,48]. Moreover, CDK6 was also inversely correlated with miR-138 in glioma tissues. Besides, we first reported that E2F2 and E2F3 were direct targets of miR-138 in glioma. However, E2F2 and E2F3 may not play critical function in miR-138-induced glioma inhibition, because of that expression of E2F3, not like EZH2, was much lower in glioma cells compared with NNB samples, and that E2F2 and E2F3 did not exhibit a negative association with miR-138. Additionally, EGFR, which is recognized as a key oncoprotein in glioma [49], was also inhibited by miR-138 and was negatively associated with miR-138 levels, which could help explain the inhibitory effect of miR-138 on glioma. Hence, our data revealed that through targeting EZH2 and CDK6 and other molecules, miR-138 played a critical role in GBM cell proliferation and tumor growth.

The classical CDK4/6-pRb-E2Fs pathway plays a crucial role in G1/S transition of cell cycle and actually, alternation of CDK4/6-pRb-E2Fs pathway is among the most common aberrations found in human glioma with CDK4/6 over-expression, Rb mutation or silencing, or E2F1 activation, resulting in deregulated glioma cell proliferation [18–20,22,50]. Coinciding with G1/S transition arrest of cell cycle, protein expressions of this pathway were obviously suppressed by miR-138, similar to siEZH2. However, these proteins were not predicted as targets of miR-138 by TargetScan or other software, implicating that knockdown of EZH2 by miR-138 eventually led to reduction of these molecules. Moreover, expression of EZH2 was down-regulated after knockdown of E2F1 and CDK4 by siRNA, although siCDK6 appeared not to alter EZH2 expression. Meanwhile, correlation analysis of gene expression from GBM samples showed that EZH2 was significantly associated with cell cycle-promoting molecules (Fig. 6), which strongly suggested that EZH2 was intrinsically involved in cell cycle control. As mentioned above, EZH2 acted as an essential downstream mediator of transcriptional factor E2F1 [21,51]. In addition, it's been considered that uncontrolled cell growth is an invariable characteristic of human cancer and that tumor cell proliferation is sustained in the

absence of growth factors [52]. Herein, it was rational that there was an EZH2-mediated CDK4/6-pRb-E2F1 signal loop, promoting glioma persistent proliferation and progression. Together, our results suggest that miR-138 acts as tumor suppressor though directly inhibiting EZH2-CDK4/6-pRb-E2F1 signal loop, blocking which by miR-138 was beneficial for tumor growth inhibition and cell cycle control (Fig. 6F).

To date, how EZH2 positively regulates its downstream molecules remains unclear. Although phosphorylation of EZH2 by Akt and CDK1/2 probably helps to explain the mechanism [53,54], it makes sense that EZH2 positively regulates CDK4/6-pRb-E2Fs by silencing their upstream tumor suppressors. However, expression levels of CDK4/6 inhibitors, such as CDKN1A, CDKN2A, Rb1 and p53 were not evaluated in this study. Correlation analysis indicated that EZH2 was negatively related with CDKN1A expression, which was similar to one study that EZH2 could repress CDKN2A to promote cell cycle progression. This may account for reduction of CDK4/6-pRb-E2Fs signals after EZH2 interference in glioma [21]. Meanwhile, EZH2 was shown to marginally correlated with P53 level in GBM (Supplementary Fig. 2), we speculated that EZH2 exerted its tumor inhibitory impact through P53 independent pathway.

In summary, we investigated the potential role of miR-138 in GBM tumorigenicity and cell cycle progression. Our findings suggest that miR-138 acts as a tumor suppressor in GBM and implicates a potential application in GBM therapy.

## Author contributions

Ying Peng conceived and designed the whole research project. Shuwei Qiu and Daquan Huang performed research work, and Fangcheng Li and Xiangping Li performed some research work. Deling Yin and Hsiang-fu Kung analyzed data. Shuwei Qiu, Daquan Huang and Ying Peng wrote the paper with important contributions from Deling Yin, Fangcheng Li, Xiangping Li and Hsiang-fu Kung.

## Acknowledgments

We thank James Elliott Denney for revision of typographical and grammatical errors in our manuscript, and thank Lina Lin and Weiyi Xu for their kind help with our work. This work was supported by Grants from the National Natural Science Foundation of China (NSFC, 81272197, 30973479 and 31070953 to Ying Peng), Oversea Collaboration Grant of NSFC, China (81228010 to Ying Peng) and International Collaboration Program of Universities in Guangdong Province (2012gjhz001 to Ying Peng).

## Appendix A. Supplementary data

Supplementary data to this article can be found online at http://dx.doi.org/10.1016/j.bbadis.2013.05.015.

## References

[1] P.H. Huang, A.M. Xu, F.M. White, Oncogenic EGFR signaling networks in glioma, Sci. Signal. 2 (87) (2009).
[2] M. Preusser, et al., Current concepts and management of glioblastoma, Ann. Neurol. 70 (1) (2011) 9–21.
[3] D.P. Bartel, MicroRNAs: genomics, biogenesis, mechanism, and function, Cell 116 (2) (2004) 281–297.
[4] M. Inui, G. Martello, S. Piccolo, MicroRNA control of signal transduction, Nat. Rev. Mol. Cell Biol. 11 (4) (2010) 252–263.
[5] K. Asadi-Moghaddam, E.A. Chiocca, S.E. Lawler, Potential role of miRNAs and their inhibitors in glioma treatment, Expert. Rev. Anticancer. Ther. 10 (11) (2010) 1753–1762.
[6] A.G. Bader, D. Brown, M. Winkler, The promise of microRNA replacement therapy, Cancer Res. 70 (18) (2010) 7027–7030.
[7] B. Kefas, et al., MicroRNA-7 inhibits the epidermal growth factor receptor and the Akt pathway and is down-regulated in glioblastoma, Cancer Res. 68 (10) (2008) 3566–3572.
[8] R.J. Webster, et al., Regulation of epidermal growth factor receptor signaling in human cancer cells by microRNA-7, J. Biol. Chem. 284 (9) (2009) 5731–5741.
[9] B. Kefas, et al., The neuronal microRNA miR-326 acts in a feedback loop with notch and has therapeutic potential against brain tumors, J. Neurosci. 29 (48) (2009) 15161–15168.
[10] B. Kefas, et al., Pyruvate kinase M2 is a target of the tumor-suppressive microRNA-326 and regulates the survival of glioma cells, Neuro Oncol. 12 (11) (2010) 1102–1112.
[11] G. Gabriely, et al., Human glioma growth is controlled by microRNA-10b, Cancer Res. 71 (10) (2011) 3563–3572.
[12] F. Crea, E.M. Hurt, W.L. Farrar, Clinical significance of polycomb gene expression in brain tumors, Mol. Cancer 9 (2010) 265.
[13] M.L. Suva, et al., EZH2 is essential for glioblastoma cancer stem cell maintenance, Cancer Res. 69 (24) (2009) 9211–9218.
[14] F. Orzan, et al., Enhancer of zeste 2 (EZH2) is up-regulated in malignant gliomas and in glioma stem-like cells, Neuropathol. Appl. Neurobiol. 37 (4) (2011) 381–394.
[15] R. Margueron, D. Reinberg, The polycomb complex PRC2 and its mark in life, Nature 469 (7330) (2011) 343–349.
[16] J.A. Simon, C.A. Lange, Roles of the EZH2 histone methyltransferase in cancer epigenetics, Mutat. Res. 647 (1–2) (2008) 21–29.
[17] T. Tonini, et al., Importance of Ezh2 polycomb protein in tumorigenesis process interfering with the pathway of growth suppressive key elements, J. Cell. Physiol. 214 (2) (2008) 295–300.
[18] K. Michaud, et al., Pharmacologic inhibition of cyclin-dependent kinases 4 and 6 arrests the growth of glioblastoma multiforme intracranial xenografts, Cancer Res. 70 (8) (2010) 3228–3238.
[19] H.Z. Chen, S.Y. Tsai, G. Leone, Emerging roles of E2Fs in cancer: an exit from cell cycle control, Nat. Rev. Cancer 9 (11) (2009) 785–797.
[20] M.M. Alonso, et al., Expression of transcription factor E2F1 and telomerase in glioblastomas: mechanistic linkage and prognostic significance, J. Natl Cancer Inst. 97 (21) (2005) 1589–1600.
[21] A.P. Bracken, et al., EZH2 is downstream of the pRB-E2F pathway, essential for proliferation and amplified in cancer, EMBO J. 22 (20) (2003) 5323–5335.
[22] S. Polager, D. Ginsberg, E2F — at the crossroads of life and death, Trends Cell Biol. 18 (11) (2008) 528–535.
[23] J.Q. Camara-Quintana, R.T. Nitta, G. Li, Pathology: commonly monitored glioblastoma markers: EFGR, EGFRvIII, PTEN, and MGMT, Neurosurg. Clin. N. Am. 23 (2) (2012) 237–246, (viii).
[24] Y. Wang, et al., MicroRNA-138 modulates DNA damage response by repressing histone H2AX expression, Mol. Cancer Res. 9 (8) (2011) 1100–1111.
[25] P. Rivetti di Val Cervo, et al., p63-microRNA feedback in keratinocyte senescence, Proc. Natl. Acad. Sci. U. S. A. 109 (4) (2011) 1133–1138.
[26] G. Siegel, et al., A functional screen implicates microRNA-138-dependent regulation of the depalmitoylation enzyme APT1 in dendritic spine morphogenesis, Nat. Cell Biol. 11 (6) (2009) 705–716.
[27] S.U. Morton, et al., microRNA-138 modulates cardiac patterning during embryonic development, Proc. Natl. Acad. Sci. U. S. A. 105 (46) (2008) 17830–17835.
[28] T. Kisliouk, S. Yosefi, N. Meiri, MiR-138 inhibits EZH2 methyltransferase expression and methylation of histone H3 at lysine 27, and affects thermotolerance acquisition, Eur. J. Neurosci. 33 (2) (2011) 224–235.
[29] L. Jiang, et al., Downregulation of the Rho GTPase signaling pathway is involved in the microRNA-138-mediated inhibition of cell migration and invasion in tongue squamous cell carcinoma, Int. J. Cancer 127 (3) (2008) 505–512.
[30] X. Liu, et al., MicroRNA-138 suppresses epithelial-mesenchymal transition in squamous cell carcinoma cell lines, Biochem. J. 440 (1) (2011) 23–31.
[31] T. Song, et al., MiR-138 suppresses expression of hypoxia-inducible factor 1alpha (HIF-1alpha) in clear cell renal cell carcinoma 786-O cells, Asian Pac J Cancer Prev 12 (5) (2011) 1307–1311.
[32] W. Wang, et al., MiR-138 induces cell cycle arrest by targeting cyclin D3 in hepatocellular carcinoma, Carcinogenesis 33 (5) (2012) 1113–1120.
[33] F. Zheng, et al., The putative tumour suppressor microRNA-124 modulates hepatocellular carcinoma cell aggressiveness by repressing ROCK2 and EZH2, Gut 61 (2) (2012) 278–289.
[34] Q. Wang, et al., Alterations of microRNAs in cisplatin-resistant human non-small cell lung cancer cells (A549/DDP), Exp. Lung Res. 37 (7) (2011) 427–434.
[35] M. Seike, et al., MiR-21 is an EGFR-regulated anti-apoptotic factor in lung cancer in never-smokers, Proc. Natl. Acad. Sci. U. S. A. 106 (29) (2009) 12085–12090.
[36] S. Mitomo, et al., Downregulation of miR-138 is associated with overexpression of human telomerase reverse transcriptase protein in human anaplastic thyroid carcinoma cell lines, Cancer Sci. 99 (2) (2008) 280–286.
[37] X. Zhao, et al., miR-138 might reverse multidrug resistance of leukemia cells, Leuk. Res. 34 (8) (2010) 1078–1082.
[38] D. Li, et al., Grade-specific expression profiles of miRNAs/mRNAs and docking study in human grade I-III astrocytomas, Omics 15 (10) (2011) 673–682.
[39] X.H. Chan, et al., Targeting glioma stem cells by functional inhibition of a prosurvival oncomiR-138 in malignant gliomas, Cell Rep. 2 (3) (2012) 591–602.
[40] P. Brescia, C. Richichi, G. Pelicci, Current strategies for identification of glioma stem cells: adequate or unsatisfactory? J. Oncol. 2012 (2012) 376894.
[41] L. Jiang, et al., miR-182 as a prognostic marker for glioma progression and patient survival, Am. J. Pathol. 177 (1) (2010) 29–38.
[42] C. Tucker-Burden, et al., Lectins identify glycan biomarkers on glioblastoma-derived cancer stem cells, Stem Cells Dev. 21 (13) (2012) 2374–2386.
[43] C.J. Chang, M.C. Hung, The role of EZH2 in tumour progression, Br. J. Cancer 106 (2) (2011) 243–247.

[44] M. Smits, et al., miR-101 is down-regulated in glioblastoma resulting in EZH2-induced proliferation, migration, and angiogenesis, Oncotarget 1 (8) (2010) 710–720.
[45] J. Lu, et al., MiR-26a inhibits cell growth and tumorigenesis of nasopharyngeal carcinoma through repression of EZH2, Cancer Res. 71 (1) (2011) 225–233.
[46] W.R. Wiedemeyer, et al., Pattern of retinoblastoma pathway inactivation dictates response to CDK4/6 inhibition in GBM, Proc. Natl. Acad. Sci. U. S. A. 107 (25) (2010) 11501–11506.
[47] J. Silber, et al., miR-124 and miR-137 inhibit proliferation of glioblastoma multiforme cells and induce differentiation of brain tumor stem cells, BMC Med. 6 (2008) 14.
[48] J. Pierson, et al., Regulation of cyclin dependent kinase 6 by microRNA 124 in medulloblastoma, J. Neurooncol. 90 (1) (2008) 1–7.
[49] S. Berezowska, J. Schlegel, Targeting ErbB receptors in high-grade glioma, Curr. Pharm. Des. 17 (23) (2011) 2468–2487.
[50] C. Atlas, Comprehensive genomic characterization defines human glioblastoma genes and core pathways, Nature 455 (7216) (2008) 1061–1068.
[51] Z.L. Wu, et al., Polycomb protein EZH2 regulates E2F1-dependent apoptosis through epigenetically modulating Bim expression, Cell Death Differ. 17 (5) (2010) 801–810.
[52] D. Hanahan, R.A. Weinberg, The hallmarks of cancer, Cell 100 (1) (2000) 57–70.
[53] T.L. Cha, et al., Akt-mediated phosphorylation of EZH2 suppresses methylation of lysine 27 in histone H3, Science 310 (5746) (2005) 306–310.
[54] S. Chen, et al., Cyclin-dependent kinases regulate epigenetic gene silencing through phosphorylation of EZH2, Nat. Cell Biol. 12 (11) (2010) 1108–1114.